FERMILAB-CONF-08-688-PPD

PHYSICS IMPACT OF THE TEVATRON *

D.C. O'NEIL

Department of Physics
Simon Fraser University,
Burnaby, BC, Canada
E-mail: doneil@sfu.ca

The Fermilab Tevatron is the highest energy, highest luminosity proton-antiproton collider ever built. It has been producing data in its "Run II" since the spring of 2001. This unique machine gives physicists at the CDF and DØ experiments access to a broad spectrum of interesting measurements and searches. The Tevatron experiments are now mature and are producing a steady stream of new results. These lectures present some of the highlights of the Tevatron programme so far, and some discussion of interesting results to come.

1. Introduction

The Fermilab Tevatron is currently the world's energy frontier machine. It has a long history, with first proton-antiproton collisions in the mid-1980s and a very successful period from 1992-1996 known as "Run I". Run I of the Tevatron led to many interesting measurements, most notably the discovery and first characterization of the top quark. From 1996-2001 the accelerator underwent an energy upgrade from 1.8 TeV to 1.96 TeV (centre-of-mass energy) and, more importantly, upgrades which allowed instantaneous luminosity gains of more than a factor of 20. At the same time, the two general-purpose collider experiments at the Tevatron (CDF and DØ), underwent substantial upgrades in order to exploit these new Tevatron capabilities. These detectors have been taking data in the so-called "Run II" since spring of 2001.

The Run II collider and detectors provide a unique opportunity to test the standard model of particle physics both through precision measurements and direct searches for new phenomena. A hadron collider at this

*This work is supported by the Natural Sciences and Engineering Research Council of Canada.

Operated by Fermi Research Alliance, LLC under Contract No. De-AC02-07CH11359 with the United States Department of Energy

energy is essentially a broadband quark and gluon collider. CDF and DØ simultaneously perform precise measurements in relatively low-transverse-momentum processes (eg. studies of B-mesons) and very high-transverse-momentum process (eg. top quark pair production). As such, the experimental output is diverse, with more than 200 published papers produced so far in Run II.

These proceedings cover a broad spectrum of Tevatron results taken from the first $2fb^{-1}$ of integrated luminosity in Run II. This broad coverage precludes presenting the intricate details of any particular analysis. Some of the results herein are precisely as presented during the 2008 Lake Louise Winter Institute (LLWI), while others are updated to reflect new results released in the weeks following the conference. The presentation of results follows that of the lectures, beginning with top quark physics, followed by studies of Ws and Zs, then by QCD, B-physics, searches for new phenomena and standard model Higgs boson searches.

2. The Top Quark

The top quark was discovered at the Tevatron in 1995 and the Tevatron experiments are still the only places in the world capable of studying its properties. The creation of top quark physics as a field of experimental study, will be the most important legacy of the Tevatron, barring evidence of new physics before the end of Run II.

The energy upgrade from Run I to Run II brings a substantial increase in the cross section for top quark production (more than 30%). This, combined with the luminosity increase, leads to relatively large samples of top quarks being available for study in Run II. Top quark mass is now a precision measurement ($< 1\%$ uncertainty) and it is now possible to measure other properties of the top quark for the first time.

2.1. *Top Quark Production and Decay*

At the Tevatron, top quarks are produced via two main mechanisms: 1) top pair production via the strong interaction and 2) single top quark production via the electroweak interaction. Some of the relevant Feynman diagrams for this process are shown in Figure 1

Due to their short lifetime relative to the characteristic timescale of the strong interaction, top quarks do not combine to form mesons, but instead decay to a W boson and a b quark virtually 100% of the time. Top quarks are also extremely massive, so their decay products are of high transverse

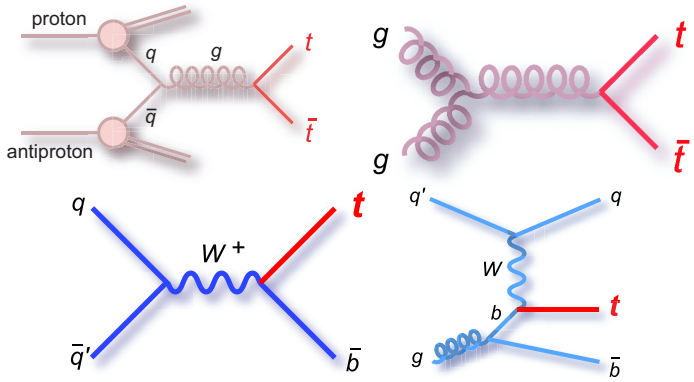

Figure 1. The first row of Feynman diagrams shows the two leading diagrams for top pair production at the Tevatron. The qq diagram on the left dominates at the Tevatron. The second row shows s-channel and t-channel EW single top quark production diagrams respectively.

momentum. This leads to final states characterized by jets or leptons from W decays and energetic b-quark jets.

Production of top quarks is still a rare process at the Tevatron, as illustrated in Figure 2. As such, background suppression through b-jet-tagging and topological constraints is essential. As discussed in the next section, multivariate techniques are also commonly used in many top quark measurements, in order to optimally extract information from the sample.

2.2. *Advanced Analysis Techniques*

As described in the previous section, top quark events are rare at the Tevatron. They can be lost amidst large standard model backgrounds, in particular from Ws produced in association with jets. Multivariate techniques are often used in order to maximally exploit a given dataset. In fact, the best measurements of top mass consistently rely on multivariate techniques, and measurement of the single top quark production cross section is simply not possible without them. For that reason, this section provides a brief description of two multivariate techniques which are becoming more common in these sorts of analyses: the matrix element method[1] and boosted decision trees[2,3].

The matrix element method is often described as a Monte Carlo (MC) event generator in reverse. A MC event generator starts from a matrix

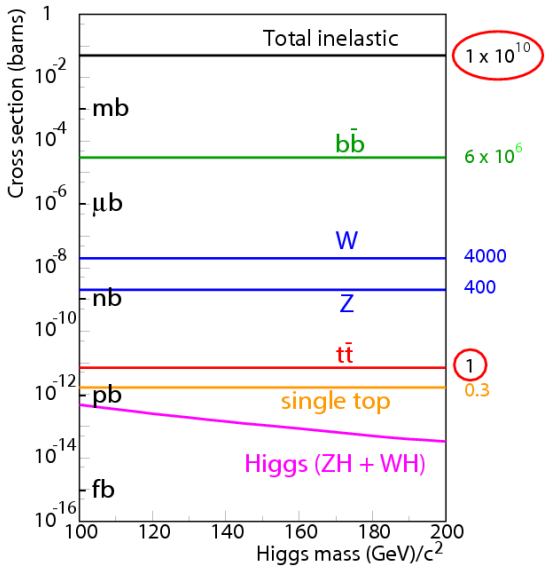

Figure 2. Theoretical predictions of top quark cross sections are presented on a log scale for comparison to other processes of interest. The axis on the right shows event rates normalized to the top pair production.

element describing the process dynamics (from Feynman Rules) which is integrated over phase space (from kinematic considerations). The integral is evaluated via a MC technique, producing specific points in phase space. The result is a set of points (events) statistically distributed as they would be in nature. The produced "particles" are then propagated through a detector simulation and a signature is produced which is (ideally) very similar to data.

A matrix element analysis starts with detector data and applies "transfer functions" to convert detector-level particle information to parton-level information. It then uses the matrix element for each process (ie. signal and each background) to calculate the probability that the given parton-level point corresponds to specific process, for example the probability that a specific set of particle 4-vectors correspond to the signal process. The inputs to this technique for each event are only the measured 4-vectors of the particles in the event. In this way the minimum set of inputs is used in a near-optimal way. The disadvantage to this technique is that a time-consuming integral must be evaluated for each event in the data sample.

A Boosted Decision Tree (BDT) is a machine-learning algorithm which turns a simple set of event selection criteria (cuts) into a powerful multivariate technique. Figure 3 shows an illustration of a simple decision

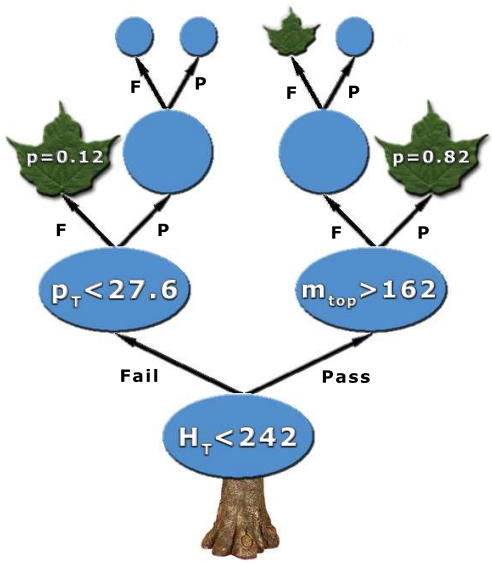

Figure 3. An illustration of a decision tree.

tree. In this illustration, the decision points (blue circles) are referred to as nodes and terminal points in the tree are drawn as leaves. The tree is grown through training the algorithm on a sample of known signal and background events. At each node, all input criteria (eg. kinematic variables) are evaluated to find the criteria and cut which best separates signal and background. The splitting of the sample stops when either a) no further separation is obtained or b) too few events remain in a given node. Each leaf of the tree is assigned a purity. Any event which passes through the tree is then assigned the purity of the leaf it stops in. This purity is the decision tree output and ranges from zero to one. If the decision tree is effective, the signal is pushed close to purity=1, while background is pushed close to purity=0.

A common way to improve the performance of a decision tree is to "boost" it. This involves training an additional set of trees which each

concentrate on a specific subset of difficult-to-classify events. At the end, the decision tree output for a given event is then a weighted average of its purity in all trees. Once the tree has been grown, it can be applied to an independent set of signal and background events to evaluate its performance.

In Figure 3, all events which have the property $H_T > 242$ pass the first cut and are subsequently evaluated at the node to the right ($m_{top} > 162$) while events which fail the first cut are subsequently evaluated at the left-node ($p_T < 27.6$). This process differs from a standard cut-based analysis in that rejected events continue to be evaluated by the algorithm in an attempt to recover lost signal.

This technique provides several advantages over other multivariate techniques including: it is fast to train, there are not many "knobs" to tune (ie. optimization is relatively simple), it is insensitive to variable correlations, and addition of extra kinematic variables will never degrade performance.

2.3. *Top Pair Production*

Since top quarks decay to Wb with branching ratio $\sim 100\%$, the final state of top quark pair production is generally described in terms of W decay channels. If both Ws decay to jets, the event is described as "all-hadronic", if one decays to an electron or a muon and the other to jets the event is described as "lepton+jets", while if both Ws decay to electrons or muons the event is described as "di-lepton". Analyses of events in which one W decays to tau (ie. τ+jets) are rare and will not be discussed here. The branching ratios for the ttbar final states are:

- all hadronic BR=46%
- lepton + jets BR=34%
- di-lepton BR=6%
- tau+X BR=14%

Generally speaking, the lepton+jets channels are the best compromise between rate and ease-of-analysis (because of the well-isolated lepton). However, different channels are subject to different systematic uncertainties and dominant backgrounds. Therefore, measurements are performed in parallel in all of these decay channels.

Top pair events have some kinematic features which are exploited in many analyses. The events are central, spherical and contain several high-transverse-momentum objects (leptons and jets). Some common variables include:

- the number of energetic jets and leptons
- H_T - the scalar sum of the transverse energies of several objects in the event
- event shape
- missing transverse energy ($\not\!\!E_T$)
- number of jets which are b-tagged

For some analyses (eg. cross section), a cut-based approach using such variables is viable. For others, multi-variate techniques (see above) must be used to produce a competitive measurement.

2.3.1. *Top Pair Cross Section*

The first priority for top-quark analyzers in Run II was to re-establish the top signal in the new data. In the years since Run II began, the uncertainty on the measurement of the top pair cross section has progressed from the Run I standard (about 25%) to a level at which it is competitive with the theoretical uncertainty (about 12%).

In May 2007, the CDF experiment released a measurement of the top pair production cross section in the lepton+jets channel based on $1.12fb^{-1}$ of Run II data[4]. They used b-jet tagging and a series of kinematic criteria to separate top pair events from backgrounds which include: W + light jets, W + heavy-flavour jets, multijets, di-bosons, single top and $Z \to \tau\tau$. The kinematic requirements include

- A single isolated lepon with $E_t > 20GeV$
- $\not\!\!E_T > 30GeV$
- 3 or more jets with $E_t > 20GeV$
- 1 or 2 b-tags
- $H_T > 250GeV$ for single-tag events, $H_T > 200GeV$ for double-tag events.

After these selections, the data composition plotted as a function of the number of jets is shown in Figure 4. The cross section was measured using

$$\sigma_{t\bar{t}} = \frac{N_{obs} - N_{bkg}}{(\epsilon_{tag} * SF)(\epsilon_{pretag} \int \mathcal{L})dt} \tag{1}$$

where N_{obs} is the number of observed events, N_{bkg} is the number of background events, ϵ_{tag} is the b-tagging efficiency, SF is a scale factor used to correct simulated b-tagging performance to data, and $\mathcal{L}$ is the luminosity.

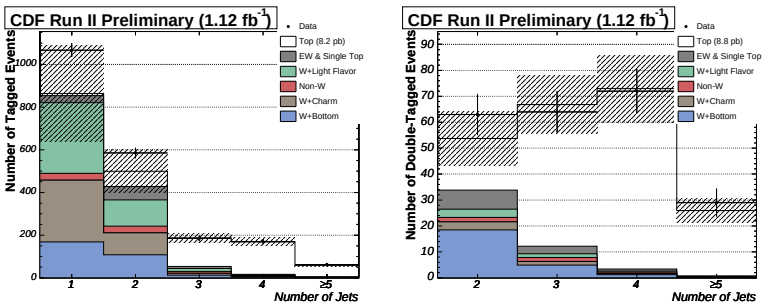

Figure 4. The predicted data composition after selection in the single-tag (left) and double-tag (right) datasets. Top pair events dominate the 3-5 jet bins.

The results for single and double-tagged events are:

$$\sigma_{t\bar{t}}(\text{singletag}) = 8.2 \pm 0.5(stat) \pm 0.9(sys)pb \tag{2}$$

$$\sigma_{t\bar{t}}(\text{doubletag}) = 8.8 \pm 0.8(stat) \pm 1.3(sys)pb \tag{3}$$

At the time of LLWI 2008 these are the single best measurements of the top pair cross sections in both single and double-tag channels.

In January 2008, the DØ experiment published a measurement of the top pair cross section without assuming the branching ratio of $t \to Wb$ was 100%[5]. A simultaneous fit was performed to extract both $\sigma_{t\bar{t}}$ and R, where R is defined as

$$R = \frac{BR(t \to Wb)}{BR(t \to Wq)} = \frac{|V_{tb}|^2}{|V_{td}|^2 + |V_{ts}|^2 + |V_{tb}|^2} \tag{4}$$

The results for $0.9fb^{-1}$ of Run II data are

$$\sigma_{t\bar{t}} = 8.2 \pm 0.9(stat + sys) \pm 0.5(lumi)pb \tag{5}$$

$$R = 0.97^{+0.09}_{-0.08}pb \tag{6}$$

The top pair cross section has been measured independently in many channels in each of the Tevatron experiments. The measurements are, in all cases, consistent with standard model predictions. The most precise measurements from each experiment are made in the lepton+jets channel. The uncertainty on a single measurement is now comparable to the theoretical precision.

2.3.2. *Top Mass*

The mass of the top quark is one of the free parameters of the standard model. Precision measurement of its value has a strong influence on the the predicted Higgs boson mass, obtained through fits to electroweak parameters[6]. As data accumulates, the measurement of the top quark mass has moved from being limited by statistical uncertainties to being systematics-dominated. In particular, the measurement precision is limited by the experimental knowledge of the jet energy scale.

As in the case of top cross section, the top mass is measured independently in many channels by each experiment. The event selection is similar to that used in the cross section analysis as well. However, the most precise single measurements of top mass typically rely on a multivariate technique and in-situ calibration of the jet energy scale. At this time, the best measurement from each experiment uses a matrix element technique in the lepton+jets channel. Figure 5 presents a summary of top mass measurements from both the CDF and DØ experiments, including results released shortly after the LLWI.

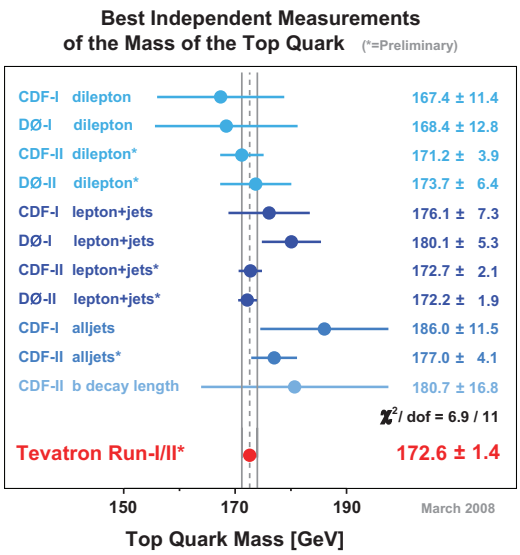

Figure 5. Summary of measurements of the top quark mass from both Tevatron experiments in Run I and Run II.

2.4. *Single Top Quark Production*

It is also possible to produce top quarks singly via the electroweak interaction. Single top quark production is interesting for a number of reasons:

- the cross section is proportional to $|V_{tb}|^2$
- the cross section is sensitive to several sources of physics beyond the standard model
- the produced top quarks are 100% polarized
- the final state is identical to an important Higgs search channel at the Tevatron
- the cross section is small, making it an excellent test-case for extracting small signals from large backgrounds

Kinematically, single top quark production lies between W+jets production and $t\bar{t}$ production and therefore suffers both as backgrounds. For this reason, it is significantly harder to measure than $t\bar{t}$ and had escaped detection until very recently. Near the end of 2006, the DØ experiment announced first evidence for single top quark production[7,8]and the first measurement of $|V_{tb}|$

$$\sigma = 4.9 \pm 1.4pb \tag{7}$$

$$0.68 < |V_{tb}| < 1.0, 95\%conf. \tag{8}$$

In the summer of 2007 CDF followed suit, and just after LLWI 2008 they released a measurement[9] which uses $2.2fb^{-1}$ of Run II data:

$$\sigma = 2.2 \pm 0.7pb \tag{9}$$

$$|V_{tb}| = 0.88 \pm 0.14(exp) \pm 0.07(theory) \tag{10}$$

Each experiment used multivariate techniques to achieve first evidence. The DØ experiment used boosted decision trees, matrix element and Bayesian neural networks while CDF used matrix elements, neural networks and likelihood methods.

2.5. *Top Quark Summary*

Run II has provided the CDF and DØ experiments with substantially larger top quark samples than were available from Run I. This has allowed precision measurement of top quark cross section and mass and first evidence of single top quark production. The precision on top mass already exceeds pre-run expectations. Many other measurements have been made in the top quark sector including: top quark charge, W helicity from top decays,

resonance searches, top width, etc. The era of precision study of top quarks is well underway.

3. Electroweak Studies

The Tevatron provides large samples of W and Z bosons, useful for studying the electroweak interaction. One of the most important parameters to measure with greater precision is the mass of the W boson, currently the limiting factor in predicting the Higgs mass within the standard model. The Tevatron also provides the first opportunity to study some types of triple gauge couplings (TGCs) through first observation of some di-boson processes.

3.1. *W Mass and Width*

Even though the mass of the W boson has been measured to high precision by the LEP experiments, its uncertainty is stills limits the prediction of the Higgs mass. The Higgs boson (or other new physics) contributes to the W boson mass through loop corrections

$$M_W = \frac{\pi \alpha_{em}}{\sqrt{2} G_f \sin^2 \theta_W (1 - \Delta r)} \tag{11}$$

where α_{em} is the fine structure constant, G_f is the Fermi constant, θ_W is the Weinberg angle and Δr is the contribution from radiative corrections.

The measurement of the W boson mass is usually performed by looking only at the leptonic W decays (ie. electrons and muons) and by constructing mass templates in two variables: W transverse mass and lepton P_t. Each of these variables is sensitive to mass, but they are sensitive to different systematic effects. For example, the lepton P_t is more sensitive to effects from hadronic recoil in the W system than is transverse mass. For this reason, the analysis is performed in each variable separately.

Improving the current knowledge of the W boson mass is a task requiring heroic effort to calibrate the detector and reduce systematic uncertainties. Early in 2007, the CDF experiment published the first W boson mass measurement of Run II[10]:

$$80413 \pm 34(stat) \pm 34(sys) = 80413 \pm 48 MeV \tag{12}$$

which is the single best measurement of W boson mass in the world. It is worth noting that this result relied on only $200pb^{-1}$ of data. As further data is analyzed, the ultimate precision on the W boson mass from Run II

could reach 20-25MeV. CDF has also measured the W boson width to be 2050 ± 59MeV which is also the world's best single measurement.

3.2. *Electroweak Fits and the Mass of the Higgs*

Given the W and top mass results presented in the previous sections, it is possible to calculate new limits on the standard model Higgs mass. The current preferred value for the Higgs mass is

$$M_H = 87^{+36}_{-27}\text{GeV} \tag{13}$$

leading to an upper limit (95% confidence) of 160 GeV. This is illustrated in Figure 6.

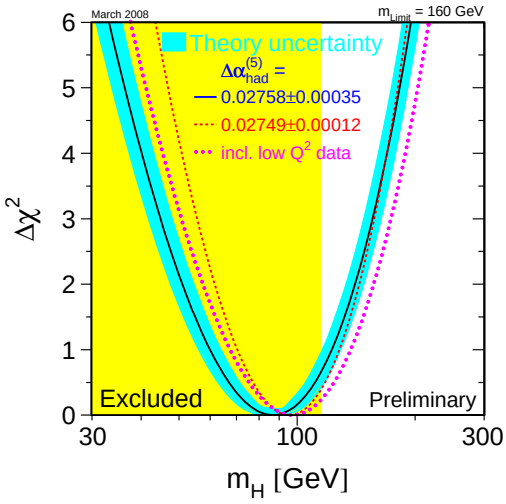

Figure 6. The latest (winter 2008) χ^2 fit to electroweak precision data. The minimum represents the favoured value for the Higgs boson mass. The shaded (yellow) region is excluded by direct searches.

3.3. *Di-boson Production*

The data of Run II also provides access to samples of di-boson events large enough to measure some cross sections for the first time. These measurements will eventually lead to new constraints on triple gauge couplings. As

data accumulates, more low-rate processes are measured for the first time. Figure 7 shows the cross sections of the di-boson processes measured so far in Run II.

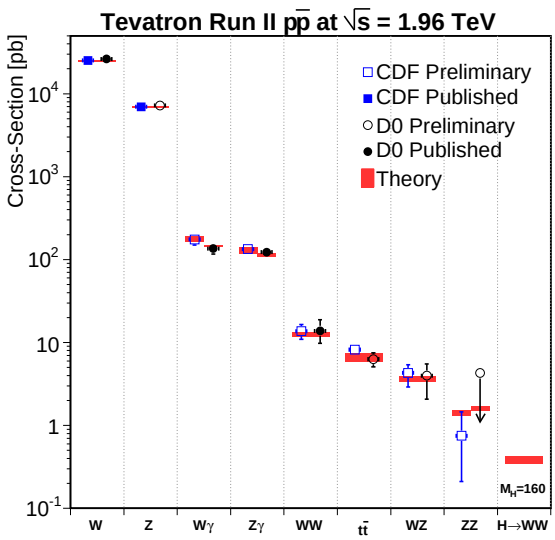

Figure 7. Measured cross section of various di-boson channels at the Tevatron.

4. QCD Studies

Many of the measurements discussed so far have actually been tests of predictions of QCD. After all, each of these processes starts from interactions of quarks and gluons, so their cross sections cannot be calculated without good experimental data on parton density functions. Many of the rare processes studied at the Tevatron are also plagued by backgrounds from di-jet production, the precise understanding of which is also a study of QCD. Studies which lead to a better understanding of jets and of QCD are an important part of the Tevatron programme.

As illustrated in Figure 8, the Tevatron explores a region in the Q^2 vs. x plane which is inaccessible to other colliders (high-Q^2, low x). This allows the Tevatron experiments to make stringent constraints on proton PDFs. Those constraints require the measurement of the differential jet

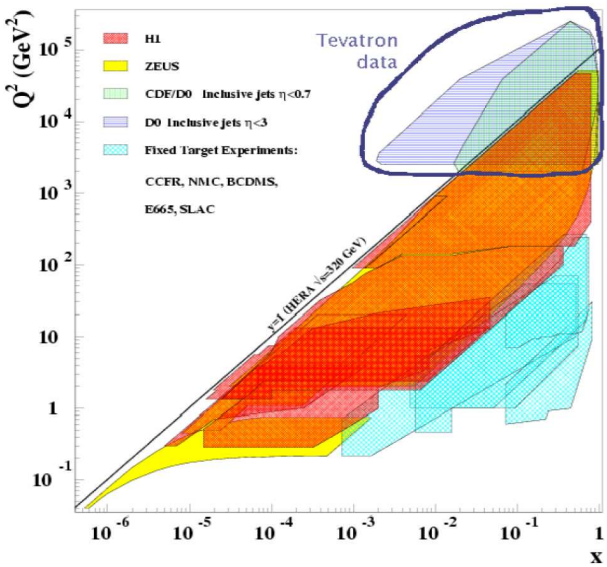

Figure 8. The Q^2 vs. x plane shows the region in which the Tevatron can constrain parton density functions.

cross section as a function of jet P_T over a large energy range. In turn, this requires unprecedented control over systematic uncertainties related to the jet energy scale. During this conference, the DØ experiment submitted new results[11] with the smallest experimental uncertainties to date. These results are shown in Figure 9.

5. B Physics

The Tevatron is not usually referred to as a B-factory, yet the cross section for production of B-hadrons is very high, and the B-physics analyzers at the Tevatron are extremely prolific (more than 50 papers published in Run II alone). The Tevatron experiments have an advantage over B-factories operating at the $\Upsilon(4S)$ resonance in that a full spectrum of B-hadrons is produced. The study of the B_s system, including mixing and CP-violation studies, is therefore a flagship measurement of the Run II programme. The Tevatron experiments also produced several other world-leading B-physics measurements, including the first observation of several new hadrons.

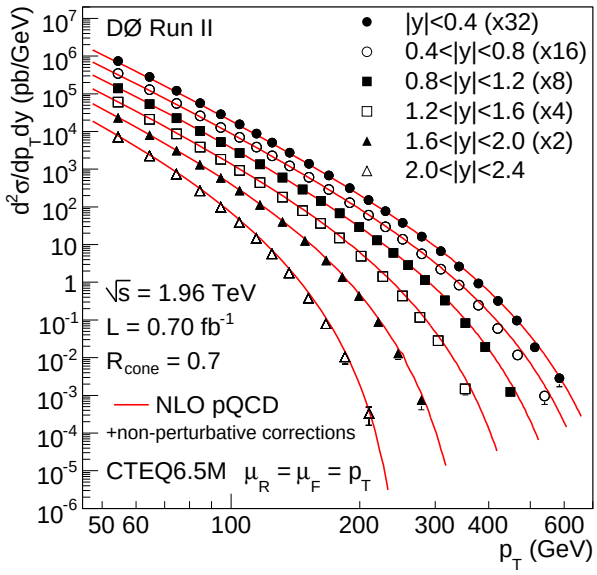

Figure 9. DØ inclusive jet cross section result. The differential cross section is plotted as a function of jet p_T in a series of rapidity bins.

5.1. B_s *Mixing*

In the B_s system, mixing between the particle and antiparticle states can occur via the box diagram shown in Figure 10.

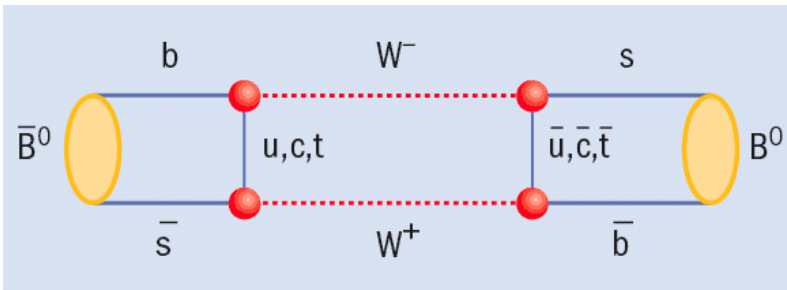

Figure 10. Feynman diagram illustrating mixing in the B_s system.

Measuring this mixing is difficult, as it is predicted to occur with very high frequency. The type of analysis needed to measure the oscillation

frequency of such a process is quite different from the high-transverse-momentum signatures described in previous sections. If an oscillation is going to be measured, the decay chain needs to be reconstructed. Further, the initial flavour of the B_s meson (ie. at production) must be determined.

Figure 11 presents a conceptual drawing of a B_s event. Here a b-quark hadronizes and forms 2 B-mesons plus other hadrons. The initial flavor of the B_s meson (matter or antimatter) can be determined either through measuring the properties of the "other" B-meson in the event (opposite-side tagging) or through charge correlations between the B_s meson and the nearest pion in the fragmentation chain (same-side tagging). In this diagram, the proper time is expressed in terms of the length L_{xy}.

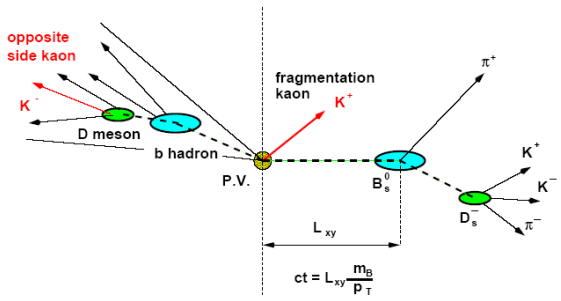

Figure 11.

In 2006, the CDF experiment published the first observation of $B_s - \overline{B_s}$ oscillations[12] and the first measurement of the oscillation frequency. The probability that the B_s meson decays with the same, or opposite flavour as the flavour at production is measured as a function of the proper time. Figure 12 shows a scan of the oscillation amplitude as a function of frequency. The amplitude is expected to be consistent with 1 when the probed frequency is the true frequency[13]. There is clear evidence of such a spike in observed amplitude. From this, CDF has extracted the oscillation frequency:

$$\Delta m_s = 17.77 \pm 0.10(stat) \pm 0.07(sys) \tag{14}$$

This measurement adds significant constraints on the CKM matrix. It constrains the ratio of 2 CKM matrix elements as follows:

$$\frac{|V_{td}|}{|V_{ts}|} = 0.2060 \pm 0.0007(exp)^{+0.0081}_{-0.0060}(theory) \tag{15}$$

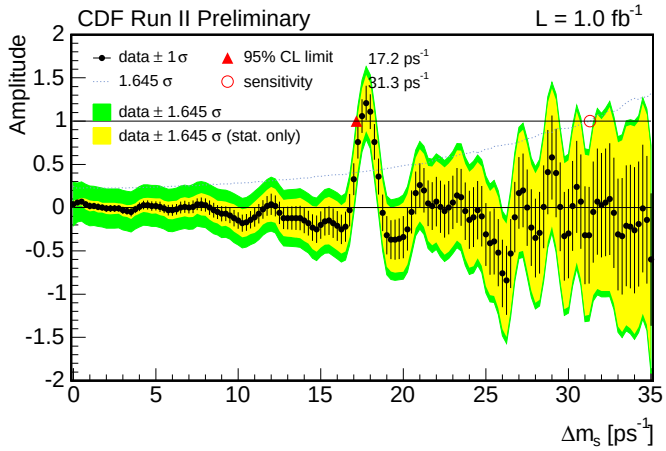

Figure 12. CDF measurement of B_s mixing amplitude. Reproduced from

These results are consistent with the standard model.

5.2. *CP-Violating Phase in B_s Mixing*

Another way to exploit the B_s system is to search for non-standard-model sources of CP violation in B_s decays. In this system, the two mass eigenstates are predicted to be almost perfect eigenstates of CP. Therefore, any measurable source of CP violation in the B_s system is a sign of new physics. The CP violation would express itself through a reduction of the difference in the widths of the 2 states. Both Tevatron experiments have made measurements of this width difference[14],[15]

$$D\emptyset \ : \Delta\Gamma_s = 0.13 \pm 0.09 ps^{-1} \tag{16}$$

$$CDF : \Delta\Gamma_s = 0.076^{+0.059}_{-0.063}(stat) \pm 0.006(syst) ps^{-1} \tag{17}$$

Both experiments are also searching for direct CP violation in B_s decays.

6. BSM Searches

In some sense, every new measurement is a search for new physics. Sometimes this is accomplished via precision measurement of standard model parameters, other times through direct production of new states. At the Tevatron, it may be possible to directly produce new particles or effects

predicted by extensions to the standard model. Until the Large Hadron Collider (LHC) begins operation, the Tevatron is the only facility capable of exploring this frontier.

6.1. *SUSY*

Supersymmetry (SUSY) refers to a new symmetry between fermions and bosons. It is reviewed extensively elsewhere[16]. SUSY has several attractive features including solving the hierarchy problem in the standard model, providing an excellent dark matter candidate (assuming R-parity conservation) and the apparent unification of couplings at high energy scales. It also has the consequence of introducing a bosonic partner for every fermion and a fermionic partner for every boson, thereby doubling the number of elementary particles in nature.

The "golden channel" for SUSY discovery at the Tevatron is 3 leptons + missing transverse energy. The $\not\!\!E_T$ comes in part from the production of the lightest supersymmetric particle (LSP). SUSY models which conserve R-Parity preclude the decay of the LSP to "normal" matter, leaving it as a weakly interacting massive particle which escapes detection. The 3-lepton + missing transverse energy signature results from quark-quark interactions producing a chargino and a neutralino. This is followed by the neutralino decay (through Z) to 2 charged leptons and an LSP, and the chargino decay (through W) to lepton + neutrino + LSP. The dominant standard model backgrounds to this process are Drell-Yann and di-boson production.

CDF has a recent result in this channel[17] which uses $2fb^{-1}$ of Run II data. The analyses are divided into two broad categories, those which require 3 isolated reconstructed leptons and those which enhance acceptance by requiring 2 isolated leptons and an isolated track. The final result is a combination of these analyses. Each analysis is an exercise in precise understanding of large backgrounds.The analyzers created 47 different control regions and tested their background model in hundreds of different distributions. The limit on the chargino mass derived from this analysis is the most stringent to date: $M_{chargino} > 140GeV$ (for mSUGRA $m_0 = 60, \tan\beta = 3, A_0 = 0, \mu > 0$). Figure 13 shows the derived limit as a function of chargino mass.

There is no a-priori reason to insist on R-parity conservation in SUSY models. If SUSY particles can decay to standard model particles, then a single slepton can decay to a lepton in violation of lepton number conservation. DØ has performed a search for this type of model through high-mass

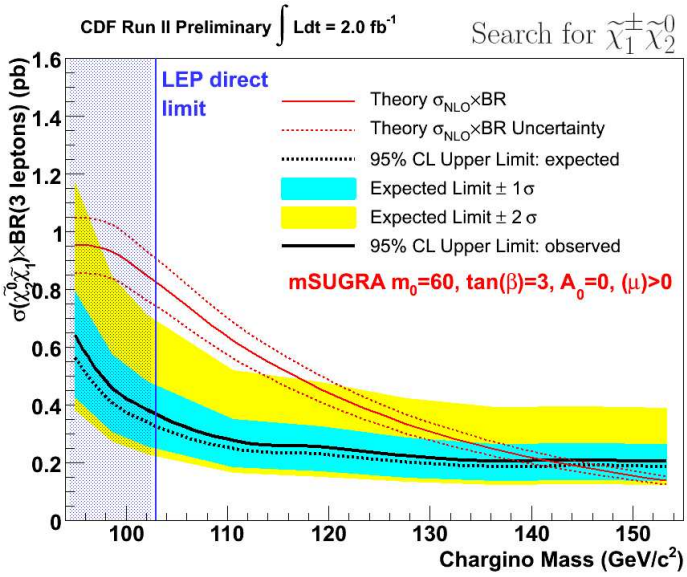

Figure 13. CDF limits on the SUSY trilepton cross section as a function of chargino mass.

$e\mu$ resonances[18]. Figure 14 shows the limits obtained in this analysis as a function of resonance mass. These are the most stringent limits to date.

6.2. *Extra Dimension Searches*

There are several theories of physics beyond the standard model in which the hierarchy problem is solved by postulating that we live in more than 4 dimensions. Two common classes of models with testable predictions at Tevatron energies are ADD (Arkani-Hamed, Dimopoulos, Dvali) models[19], which postulate the existence of "n" large extra dimensions and Randall-Sundrum models[20] which postulate the existence of a fifth warped dimension.

CDF has released results of a search for evidence of ADD extra dimensions using $2fb^{-1}$. The process is $q\overline{q} \rightarrow \gamma + G$. The graviton is undetected, leading to a photon+MET final state. The lower limit on the ADD scale is pushed to approximately $1TeV$ for number of extra dimensions 2-6.

Randall-Sundrum theory predicts a tower of Kaluza-Klein excitations (RS-gravitons). The first of these excitations should have a mass in the TeV range. The signature would be a narrow high-mass resonance decaying to

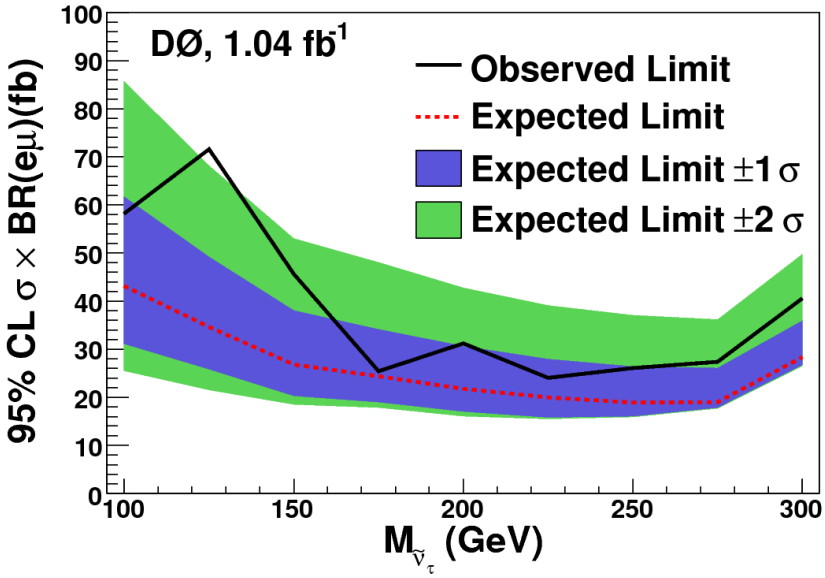

Figure 14. DØ limits on the RPV-SUSY $e\mu$ resonance cross section as a function of resonance mass.

pairs of fermions or bosons. DØ has done a search for ee and $\gamma\gamma$ in a sliding window from 100GeV to 1TeV in $1fb^{-1}$ of Run II data[21]. Figure 15 shows the region of phase space excluded by this result.

6.3. *Lepton Compositeness*

If leptons are composite objects, excited states can be produced. One of the decay channels for an excited electron would be $ee\gamma$. DØ has performed a search in this channel in $1fb^{-1}$ of Run II data[22]. This analysis has produced the most stringent limits yet on the mass of the excited electron: $M_{e^*} > 756GeV$ (for $\Lambda = 1TeV$)

6.4. *Searches Summary*

The Tevatron experiments have always been at the energy frontier, and so have been directly searching for new phenomena since their inception. However, CDF and DØ are now mature, with excellent understanding of the experimental environment and of standard model signatures. As such, the experiments have now entered a golden era for searches. For the moment,

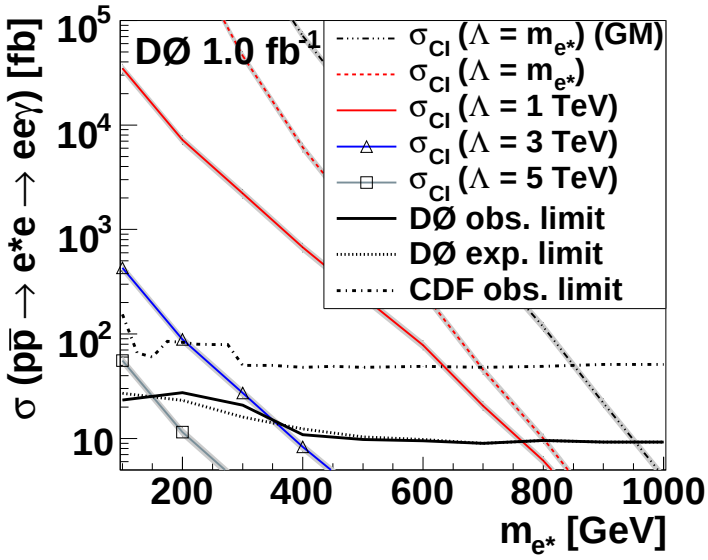

Figure 15. DØ limits on the production of ee and $\gamma\gamma$ resonances due to RS graviton production and decay.

the success of these searches can be seen through new constraints on many models of new physics. The hope, of course, is that the Tevatron will directly reveal a new secret of nature before Run II is complete.

7. Higgs Searches

Understanding electroweak symmetry breaking is one of the great quests of modern particle physics. Within the standard model, electroweak symmetry is broken via the Higgs mechanism. This predicts the existence of a massive scalar boson: the Higgs boson. Since the end of data-taking at LEP-II in 2000, the Tevatron has been the only collider capable of accessing high enough energy scales to potentially discover the Higgs boson. However, the allowed mass range for the Higgs boson is at the edge of the Tevatron reach. This means that its discovery is only feasible with high integrated luminosity. Each experiment has been increasing its focus on Higgs searches recently, making this one of the most exciting areas of study during the final years of Run II.

7.1. *Higgs Boson Production and Decay*

Figure 16 presents Feynman diagrams for the two leading Higgs boson production mechanisms at the Tevatron. The leading production mechanism is known as gluon fusion and results in production of only a Higgs boson in the final state. The second diagram is referred to as associated production, since the Higgs is produced in association with a W boson.

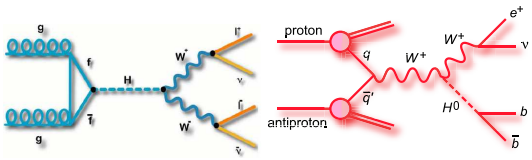

Figure 16. Feynman diagrams representing two of the leading production mechanisms for standard model Higgs bosons at the Tevatron. The diagram on the left is known as gluon fusion, while the diagram on the right is referred to as associated production.

The branching ratio for Higgs boson decays to any specific final state changes significantly as a function of Higgs mass as demonstrated in Figure 17. For Higgs masses below approximately $140 GeV/c^2$, the dominant

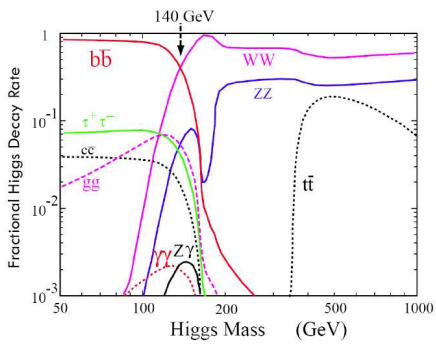

Figure 17. The branching ratio for many Higgs decay channels as a function of Higgs boson mass.

decay is to a $b\bar{b}$ pair. Unfortunately, the rate of $b\bar{b}$ di-jet production from other standard model sources is higher by many orders of magnitude. This makes associated production more attractive than gluon fusion by the virtue of smaller backgrounds to $W + H$ or $Z + H$ final states. Therefore, for low

mass Higgs the signature is (in the case of $W + H$) an isolated lepton, $\not{E}_T$ and 2 b-tagged jets. For higher Higgs masses the dominant decays are to WW and ZZ pairs and the gluon-fusion production mode becomes the most attractive channel due to its rate. For either low-mass or high-mass Higgs the analysis is very challenging, and requires precise knowledge of backgrounds and sophisticated analysis techniques.

7.2. *Current Results*

The cross section limits derived from current Higgs searches are still significantly above the standard model cross sections, typically by a factor of 10 or more over the entire mass range. However, by combining results from many channels and from both experiments it is possible to get much closer to excluding (or discovering!) the Higgs boson in some mass regimes. Figure 18[23] shows the combination of many Higgs cross section limits from the CDF and DØ experiments. From this figure it is clear that currently the best chance to find or exclude the existence of the Higgs is in the region of $M_H = 160GeV$ (where WW decays dominate).

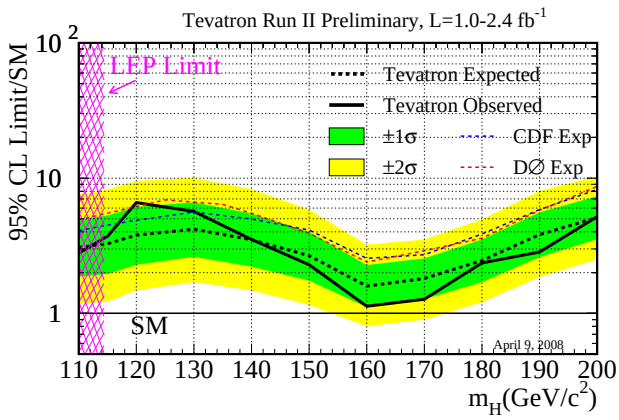

Figure 18. The ratio of the Higgs boson cross section limit to the standard model prediction plotted as a function of Higgs mass. This is a combination of many analyses from both Tevatron experiments

7.3. *Higgs Searches Summary and Prospects*

The hunt for the Higgs boson is one of the most important quests in particle physics. The Tevatron experiments are pouring effort into the search and are now approaching sensitivity to standard model cross sections in some parts of the allowed Higgs mass range. As more data is accumulated, analysis techniques are refined, and new channels are explored the sensitivity will continue to improve. A 2003 sensitivity study[24] showed that with $4fb^{-1}$ per experiment the standard model Higgs boson could be excluded up to $130GeV/c^2$ or could be seen with 3-sigma evidence up to about $120GeV/c^2$ as shown in Figure 19.

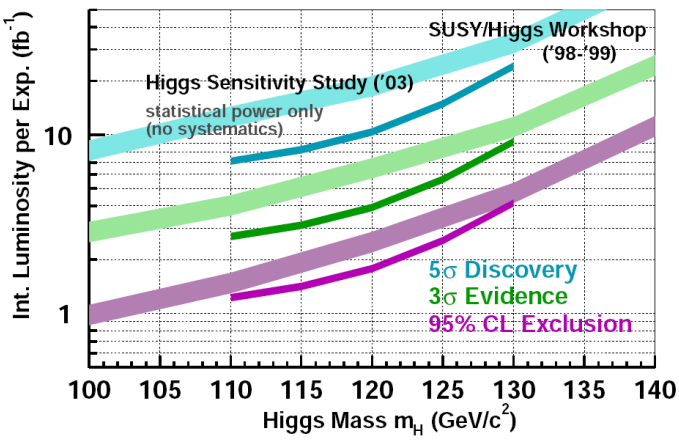

Figure 19. The predicted exclusion, evidence and discovery curves for a given luminosity (per experiment) and Higgs mass according to a 2003 study. The thick lines represent the results of a similar study performed in 1999.

8. Conclusions

Run II of the Fermilab Tevatron has been ongoing since spring of 2001. Since that time, the CDF and DØ experiments have combined to publish more than 200 papers in many different areas of particle physics. While the Tevatron will always be remembered for having opened the field of top quark physics, there have also been significant impacts on understanding the W and Z, on QCD, on B-physics, on searches for physics beyond the standard model and on searches for the standard model Higgs boson. The

detectors and experimental environments are now very well understood, and new data is accumulating at an unprecedented rate. I expect the Tevatron to continue to have an impact on our field for years to come.

References

1. V.M. Abazon et al. (D0 Collaboration) *Nature* 429, 638 (2004).
2. L. Breiman, J. Friedman, C.J. Stone, and R.A. Olshen, *Classification and Regression Trees*, Wadsworth, Stamford, 1984.
3. D. Bowser-Chao and D.L. Dzialo, Phys. Rev. D 47, 1900 (1993).
4. CDF Public Note 8795.
5. V.M. Abazov et al. (D0 Collaboration) *Phys. Rev. Lett.* 100, 192003 (2008)
6. The results of the LEP electroweak working group. *http://lepewwg.web.cern.ch/LEPEWWG/*.
7. V.M. Abazov et al. (D0 Collaboration), *Phys. Rev. Lett.* 989, 181802, 2007.
8. V.M. Abazov et al. (D0 Collaboration), Accepted to *Phys. Rev. D*, 2008, arXiv:0803.0739; Fermilab-Pub-08/056-E.
9. CDF Public Note 9251.
10. A. Aaltonen et al. (CDF Collaboration), *Phys. Rev. Lett.* 99, 151801 (2007).
11. V.M. Abazov et al. (D0 Collaboration) *Phys. Rev. Lett.*, xxxxxx (2008), arXiv:0802.2400; Fermilab-Pub-08/034-E.
12. A. Abulencia et al. (CDF Collaboration) *Phys. Rev. Lett.* 97, 242003 2006.
13. H.G. Moser and A. Roussarie, *Nucl. Instrum. Methods Phys. Res. Sect. A* 384, 491 (1997).
14. V.M. Abazov et al. (D0 Collaboration) *Phys. Rev. D* 76 , 057101 (2007)
15. T. Aaltonen et al. (CDF Collaboration) *Phys.Rev.Lett.* 100:121803 2008
16. H.P. Nilles *Phys. Rept.* 110:1-162,1984; H. Haber and G. Kane, *Phys.Rept.*117:75-263,1985; S.P. Martin hep-ph/9709356; I. Aitchison *Supersymmetry in Particle Physics* Cambridge, 2007.
17. The CDF Collaboration, CDF Public Note 9176.
18. V.M. Abazov et al, Submitted to *Phys. Rev. Lett.*, xxxxxx (2008). arXiv:0711.3207; Fermilab-Pub-07/620-E
19. N. Arkani-Hamed, S. Dimopoulos, G.R. Dvali, *Phys.Lett.B* 429:263-272,1998.
20. L. Randall, R. Sundrum, *Phys. Rev. Lett.* 83:3370-3373,1999.
21. V.M. Abazov et al. (D0 Collaboration) *Phys. Rev Lett.* 100, 091802, 2008.
22. V.M. Abazov et al. (D0 Collaboration), accepted by *Phys. Rev D Rapid Commun.*, arXiv:/0801.0877 [hep-ex], 2008.
23. Tevaton New Phenomena and Higgs Working Group Report for Winter 2008, *arXiv:0804.3423v1, FERMILAB-PUB-08-069-E*
24. Tevatron Higgs Sensitivity Study Group, *FERMILAB-PUB-03/320-E*